Density-functional theory of melting of clusters and films

S. T. Chui
Bartol Research Institute, University of Delaware, Newark, Delaware 19716
(Received 23 January 1992)

We study the melting of clusters and thin films as a mass-density-wave instability by generalizing recent density-functional methods of melting. We found that the freezing temperature is increased for thin films whereas for clusters it is decreased. For spherical boundaries, at melting the Debye-Waller factor as a function of the radial distance consists of a flat bulklike part close to the center and a decaying interface part at the surface. For small particles, the surface part dominates. This represents a type of generalized Lindemann criterion for small clusters. Our calculation also provides a detailed microscopic description of the density distribution and more physical insight about the system.

I. INTRODUCTION

Theoretical predictions of a depression in the bulk melting temperature in small particles or clusters have existed since 1909.[1] Experimental verifications of these predictions became available when Takagi made a series of melting-point-depression measurements on small particles of Pb, Sn, and Bi.[2] Since that time there have been a number of experimental[3] and theoretical investigations of the melting behavior in a variety of small particles and clusters. Following earlier work by Matsubara, Iwase, and Momkita,[4] Hasegawa, Hoshino, and Watabe[5] determined the melting temperature by comparing the free energy of the fluid state calculated using the modern theory of fluids[6] with the hard-sphere fluid as a reference system and that of the solid state calculated with a position-dependent Einstein model. Sheng, Cohen, and Schrieffer[7] investigated the finite-size effects by applying the Devonshire shell model[8] of liquid and introduced a finite-size entropy factor based on studies of the N-spin mean-field calculation.

Over the last ten years, there has been much improvement in the quantitative description of the melting process in two dimensions by focusing on the roles played by topological defects[9,10] and in three dimensions as an instability from either the solid[11] or the fluid side.[12] Whereas the early phonon instability calculations gave transition temperatures that are an order of magnitude off from the real one, recent calculations incorporating the third-order anharmonic correction as well as incorporating vacancies provided transition temperatures that agree with experimental results to within 20%. Similar improvement on the work of Kirkwood and Monroe[13] of studying the instability from the fluid side has also been obtained recently by Ramakrishnan and Yussouff[12] (RY). In this paper we generalize this approach to studying the freezing of small finite systems such as clusters and films. The melting of clusters is of interest in the study of porous materials such as Vycor and various forms of rocks and in granular metals. The melting of thin films is of interest for several reasons. In the study of tribology and lubrication, one often has a thin film of fluid between two solids. The viscosity of this film obviously depends on whether it is a solid or not. Multilayer structures made with metals or semiconductors are now commonly made in the laboratory and their melting behavior is obviously of interest. In the limit that the film thickness becomes small, one approaches the two-dimensional limit in which there has been much interest. How the two-dimensional limit is approached is not understood at the moment.

We found that the freezing temperature is increased but the mean-squared vibrational amplitude is decreased for thin films whereas for clusters the reverse is true. Physically, the plane boundary in a film suppresses density fluctuation while the boundary in a small cluster enhances density fluctuation. We interpret this as the physical origin of the opposite trends of the melting temperature for the two finite systems. Our result is consistent with recent experiments of Unruh *et al.*[14] whose result suggests that the melting temperature is increased in multilayer films of copper and tungsten while in granular systems of tin and SiO_2 they are suppressed.

We also found that at melting the Debye-Waller factor as a function of the radial distance is similar after a scaling by the cluster radius R for different cluster sizes R. This represents a type of generalized Lindemann criterion for small clusters. Our calculation provides a detailed microscopic description of the density distribution in restricted geometries both at and away from the melting temperature.

II. MELTING AS A MASS DENSITY WAVE

Many authors have considered melting as a mass-density-wave instability[13,15,16,12] where one starts off in the liquid state and ask if a density modulation can be self-consistently sustained. Mathematically, one introduces a periodic modulation for the mass density $\rho(r)$ of the form

$$\rho_s(r)=\rho_0\left[1+\eta+\sum_j \mu_j \exp(i\mathbf{K}_j\cdot\mathbf{r})\right] .$$

Here $\mathbf{K}_j$ are reciprocal-lattice vectors of the corresponding solid; the "order parameter" μ_j corresponds to the Debye-Waller factors and is equal to

$\exp[-K_j^2\langle(\delta r)^2\rangle/2]$ in the solid phase; η represents a density change on freezing. This mass density wave generates an effective potential on the fluid particles. Motivated by past studies of liquids, various approximations to calculate this potential have been proposed. The approach of Ramakrishnan and Yusouff is motivated by the hypernetted-chain approximation and, in the lowest approximation, turns out to work best. Recently Curtin and Ashcroft[17] introduced another approximation, which they consider to be more realistic, and which also works well but is more complicated to carry out. In this paper, we shall adopt the philosophy that, presumably, some of these calculations worked because there are some cancellations of higher-order terms in a way that we do not completely understand. We shall use the approach of RY because it is simpler to carry out. In this approximation, the self-consistent potential $V_s(r)$ generated by the mass density modulation is given by the hypernetted-chain approximation as

$$-\beta V_s(r)=\int dr' c(r-r')\Delta\rho(r')/\rho_0 , \tag{1}$$

where c is the direct correlation function much discussed in the study of fluids. Its Fourier transform is related to the structure factor $S(k)$ by $c(k)=1-S^{-1}(k)$. Intuitively, one can regard c as some kind of irreducible susceptibility. All the dependence of V_s on the original bare potential is contained in c. By introducing c, the dependence on the interparticle potential is now "factored out." Substituting our form for ρ and carrying out the integral over r', we obtain the effective potential

$$-\beta V_s(r)=c_0\eta+\sum_j \mu_j c(K)\exp(i\mathbf{K}_j\cdot\mathbf{r}) ,$$

where c_0 is the Fourier transform of $c(r)$ at zero wave vector. The self-consistent condition is then derived from the equation

$$\rho(r)=\rho_0\exp[-\beta V_s(r)] . \tag{2}$$

Multiplying both sides of this equation by 1 and $\exp(-iKr)$, respectively, and integrating with respect to r, we obtain

$$1+\eta=g(x)\exp(c_0\eta) , \tag{3}$$

$$\mu_j=f_j(x)\exp(c_0\eta) , \tag{4}$$

where the functions f and g are defined by

$$g(x)\exp(c_0\eta)=\int dr\exp[-\beta V_s(r)]/V ,$$

$$f_j(x)\exp(c_0\eta)=\int dr\exp(-i\mathbf{K}_j\cdot\mathbf{r})\exp[-\beta V_s(r)]/V ;$$

$x=c_1\mu_n$. The integrals g and f_j can be calculated by the Gauss-Legendre formula. With a six-point and a ten-point formula, the final results differ by less than 1%.

In general η is very small compared with one. From Eq. (3) obtain $\eta\approx\ln(g)/(1-c_0)$. Substituting into Eq. (4) we obtain

$$\mu_j=f_j g^{c_0/(1-c_0)}=F_j(x) . \tag{5}$$

The number of reciprocal-lattice vectors (RLV's) necessary for good results depends on the crystal structure involved. For the bcc lattice, keeping only the lowest RLV provides for a reasonable transition temperature. We shall restrict our attention to this case for the sake of simplicity. F_1 is shown in Fig. 1. In our calculation, we have fitted F as a polynomial in x; the details of this are discussed in the Appendix where we also discuss the graphical solution of Eq. (5).

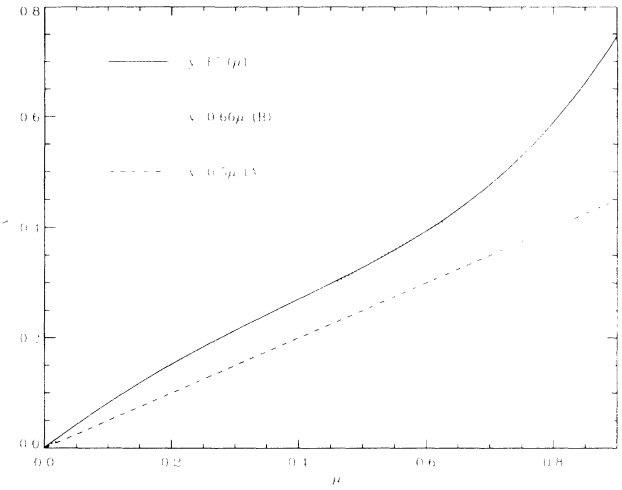

FIG. 1. Graphical solution of the instability equation [Eq. (5)]. The curve is $F^{-1}(x)$ vs x. Straight lines A and B are given by $y=c_1x$ for different c_1. The melting transition occurs when the straight line B is tangent to the curve.

III. INHOMOGENEOUS SYSTEMS

External boundaries create a change in the density distribution already in the fluid phase. Monte Carlo simulation of *fluids* close to a *plane* boundary have been performed by Liu, Kalos, and Chester,[18] by Abraham and Singh,[19] and by Snook and Henderson.[20] These authors investigated the density profile away from the plane boundary. Analytic calculations of the interface profile have been investigated by Henderson, Abraham, and Barker[21] using the Ornstein-Zernike relation and by Samm and Ebner[22] with the hypernetted-chain approximation. In this latter calculation, one focuses on a functional of the density distribution that has to be minimized. This same functional is the one used by McMullen and Oxtoby.[23]

Chui[24,25] recently carried out a Monte Carlo study of the structure of hard-sphere *solids* and fluids surrounded by *spherical* walls. He found an increase in the density of both the solid and the fluid at the wall but this increase is less than that in the case of *flat* walls.

The density profile in the fluid phase can be semiquantitatively explained by the linear theory of Henderson, Abraham, and Barker,[21] which was originally derived from consideration of pair correlation function in fluid mixtures. It starts from the Ornstein-Zernike relationship which can be obtained by linearizing Eq. (2). We get

$$\rho_w(r)=\rho_0\left[1+\int d^3r'c(r-r')\delta\rho_w(r')\right]$$
$$=\rho_0[1-\beta V_w^0(r)]\ , \tag{6}$$

where $\delta\rho_w=\rho_w-\rho_0$. Because of the wall, the new particle density must be zero outside the wall. Thus $\delta\rho=-\rho_0$ outside the spherical wall. This corresponds to an effective wall potential $-\beta V_b(r)$ in the grand canonical potential given by

$$-\beta V_b(r)=-\rho_0\int_{r'>a} d^3r'c(r-r')\ . \tag{7}$$

The total effective potential is

$$-\beta V_w(r)=-\beta V_b(r)+\int_{|r'|<a} d^3r'c(r-r')\delta\rho_w(r')\ . \tag{8}$$

The change in density due to the wall is given by

$$\delta\rho_w(r)=-\beta V_b(r)+\int_{|r'|<a} d^3r'c(r-r')\delta\rho_w(r')\ . \tag{9}$$

To study the crystal-melt interface Oxtoby and Haymet[26] have extended the approach of RY to inhomogeneous problems such that the order parameters η and μ are now functions of positions. While Oxtoby and Haymet have focused on the crystal-metal interface and infinite-size systems, the equation that they derive should still be applicable to finite-size systems, provided that the correct boundary condition is applied. Exploiting this, we have investigated the melting of finite-size clusters and thin films in this paper.

To investigate the formation of a solid in the presence of a wall, we consider a total density of the form

$$\rho_s(r)=\delta\rho_w+\rho_0\left[1+\eta(r)+\sum_j \mu_j(r)\exp(i\mathbf{K}_j\cdot\mathbf{r})\right]\ .$$

The total effective potential is now

$$-\beta V_s(r)=-\beta V_w(r)+\int_{|r'|<a} dr'c(r-r')\rho_0\left[1+\eta(r')+\sum_j \mu_j(r')\exp(i\mathbf{K}_j\cdot\mathbf{r})\right]\ . \tag{10}$$

We again made the linear approximation for $\delta\rho_w$ and arrive at the equation

$$\rho_s(r)-\delta\rho_w(r)=\rho_0\exp[-\beta(V_s-V_w)]\ . \tag{11}$$

This approximation is suggested by recent Monte Carlo (MC) simulations. In our MC simulation of hard-sphere fluids for spherical walls,[24,25] we also calculated a local structure factor defined as the structure factor averaged over particles at different distances from the origin. Similar results have not been reported for flat walls. We have carried out Monte Carlo simulations for those cases. Our results for the local structure factor, together with the density distribution, are shown in Fig. 2. Whereas the local density is increased at the wall, no corresponding increase is seen in this local structure factor in the solid phase. For spherical walls, the local structure factor is zero at the wall; for flat walls, it remains finite. This is as one would expect, because a spherical wall makes it difficult to form a solid.

That there is no dramatic increase in the local structure factor at the wall suggests that the coupling between $\delta\rho_w$ and the density change caused by the formation of the solid is small, justifying the above approximation. Equation (11), coupled with the proper boundary conditions, is the central result of the present paper. To illustrate the difference between melting in films and in clusters, we discuss below one approximate way of solving this nonlinear equation.

We follow Oxtoby and Haymet and assume that the spatial variation of the order parameters $\eta(r')$ and $\mu(r')$ are much slower than the periodic variation $\exp(i\mathbf{K}_j\cdot\mathbf{r})$ in Eq. (1). $c(r-r')$ is a short-range function with a range of the order of an atomic spacing. As we see in Figs. 2 and 3, the envelope of $S_K(r)$ varies slowly on the scale of atomic distances; thus we expect the variation of η,μ over this distance to be small. We thus expand the order parameters as a Taylor series expansion in $r'-r$ about r; retaining the lowest nontrivial order, we get

$$-\beta V_s(r)=\int dr'c(r-r')\{1+(r'-r)\nabla$$
$$+[(r'-r)\nabla]^2/2\}\eta(r)$$
$$+\sum_j \exp(i\mathbf{K}_j\cdot\mathbf{r})\{1+(r'-r)\nabla$$
$$+[(r'-r)\nabla]^2/2\}\mu_j(r)\ .$$

We next write $c(r-r')$ in terms of its Fourier transform and obtain $c(r')r_a'r_b'=-\int dk\, c(k)\partial_{ka}\partial_{kb}\exp(ikr')$. Integrating by parts, we obtain $c(r')r_a'r_b'=-\int dk[\partial_{ka}\partial_{kb}c(k)]\exp(ikr')$. Substituting this into the above equation and carrying out the r' integrations, we obtain

$$-\beta V_s(r)=\sum_j \exp(i\mathbf{K}_j\cdot\mathbf{r})[c(K)\mu_j+D(\mu_j)]$$
$$+c_0\eta-0.5c_0''\nabla^2\eta$$

because $c'(K)=0$. Here

$$D(\mu_j)=-0.5(\mathbf{K}\cdot\nabla)^2\mu_j c''(K_j)\ .$$

This so-called squared gradient approximation has been used in the study of the gas-liquid interface.[27] Because the decay length of $S_K(r)$ (Fig. 3) is of the order of several lattice constants, we expect the squared gradient approximation to be reasonable. The equation for $-\beta V_s(r)$ in spherical shells is very similar to our previous equation in films except that $\mu_j c(K)$ is now replaced by $\mu_j c(K)+D(\mu_j)$. The self-consistent equation is again given by the "Boltzmann distribution" $\rho(r)=\rho_0\exp[-\beta V_s(r)]$. The instability conditions are still given by Eqs. (3) and (4) except that x now also contain second-derivative terms. We thus arrive at the following

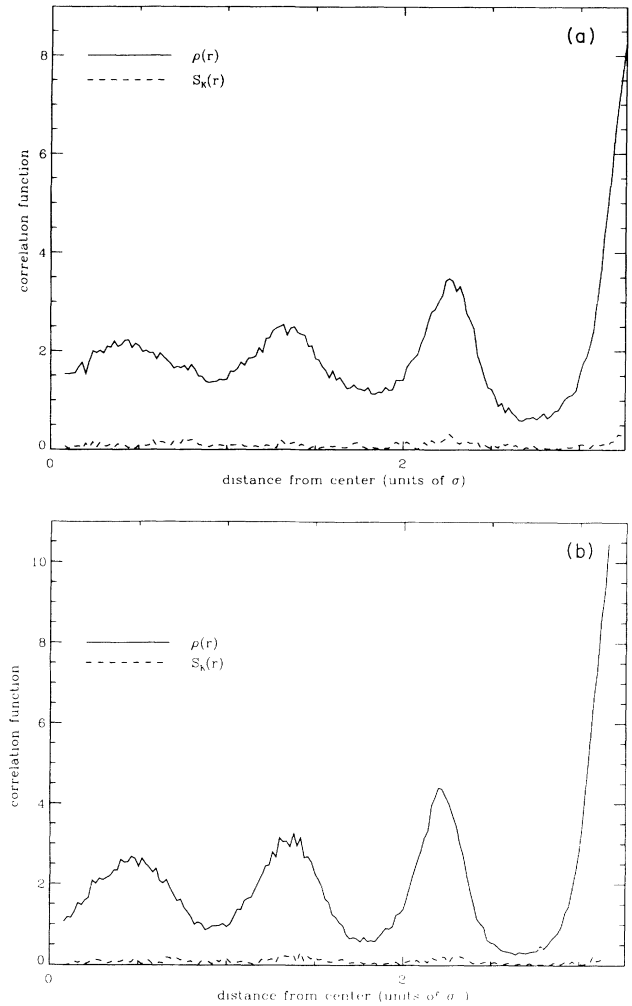

FIG. 2. The density and local structure factor away from the center with planar interfaces at $x=\pm 3.3$ for hard-sphere systems at densities of (a) 0.9 and (b) 1.0.

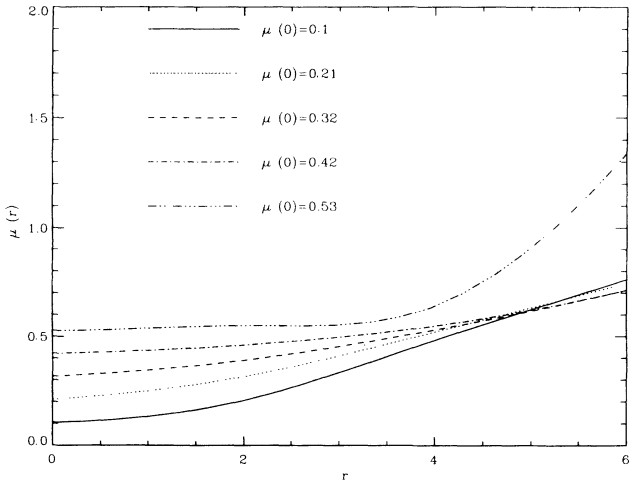

FIG. 3. The trajectory of μ as a function of r for a spherical cluster for various initial values $\mu(r=0)$. $c_1=0.63$, corresponding to a temperature above melting.

generalization:

$$1+\eta=g(c(K)\mu_j+D(\mu_j))\exp(c_0\eta-0.5c_0''\nabla^2\eta)\ , \tag{12}$$

$$\mu_j=f_j(c(K)\mu_j+D(\mu_j))\exp(c_0\eta-0.5c_0''\nabla^2\eta)\ . \tag{13}$$

Dividing these two equations, we obtain

$$\bar{F}^{-1}(\mu_j/(1+\eta))=c(K)\mu_j+D(\mu_j)\ , \tag{14}$$

where $F=f/g$. This equation determines μ' in terms of η and μ. Substituting it back, we obtain another equation for η'.

The above calculation assumes that the order parameters are functions of rectilinear coordinates x, y, and z; which is more appropriate for planar boundary conditions and thin film geometry. Harrowell and Oxtoby[28] have also investigated a spherical interface that corresponds to a droplet in the context of nucleation theory. In that case they still focus on Eqs. (3) and (4) but now the order parameters μ are assumed to be only a function of the radial distance away from the center. All order parameters that are symmetry related to one another are assumed to be identical. The Laplacian can then be written only in terms of radial derivatives. x is then given by $x_s=c_1\mu-c_1''(\mu''+2\mu'/r)/6$. The operator D is given by $D(\mu)=-c_1''(\mu''+2\mu'/r)/6$. This will also be useful to us when we consider the melting of clusters.

IV. MELTING OF CLUSTERS

The clusters can be connected or disconnected. Our calculation assumes a grand canonical ensemble and seems more appropriate for connected clusters. The difference between the grand canonical and canonical ensembles may be small for the system sizes in which we are interested but this remains to be investigated. We first consider a spherical metal cluster of finite radius and focus on the boundary conditions. For the derivative terms in x_s to remain finite at the origin, it is necessary that $\mu'(r=0)=0$. We also expect the mass density to be zero *outside* the wall; hence, approximately $\mu(R)+a\mu'(R)=0$, where a is the atomic distance. Since μ is positive, this condition can be satisfied only if μ decreases fast enough as a function of r. We solve the differential equation

$$-c_1''(\mu''+2\mu'/r)/6=F^{-1}(\mu)-c_1\mu=h(\mu)\ , \tag{15}$$

subject to the above boundary conditions. For concreteness, we illustrate our results using parameters appropriate for sodium. In that case $c_0=-40$, $c_1''=-1.156$ where the distances are expressed in units of the lattice constant. For our parametrization, melting in the bulk occurs at $c_{1m}=0.687$. We next illustrate the solution of the boundary value problem with the "shooting method" by discussing the trajectories of the order parameters with $\mu(0)=0$ and investigate if the other boundary condition can be satisfied at $r=R$ at temperatures above, close to, and below melting. For a given radius R, the transition condition is determined by the smallest value of c_1 at which our boundary conditions can no longer be satisfied no matter what the initial value $\mu(r=0)$ is.

The differential equations are solved with a sixth-order Runge-Kutta scheme. The trajectory of μ as a function of r is shown in Fig. 3 for $c_1=0.63$, corresponding to a temperature above melting. For $c_1<c_{1m}$, as we see from Fig. 1, F^{-1} is always larger than $c_1\mu$, the right-hand side of Eq. (15), $h(\mu)$, is always positive. As r is increased, μ always increases. Our boundary condition can never be satisfied. The trajectory of μ as a function of r is shown in Fig. 4 for $c_1=0.65$, corresponding to a temperature close to melting. As we can see from Fig. 1, for $\mu<0.5$, $h(\mu)$ is positive, corresponding to a positive "acceleration." This "acceleration" becomes very small for $0.5<\mu<0.6$. For $\mu>0.6$, it is positive once again. Thus in Fig. 4, if the initial value of μ is very different from 0.5, it will increase rapidly. If the value of μ is close to 0.5, it changes slowly until one is far away from this value, then it increases again. Thus it never *decreases* with a big enough slope that the boundary condition at R can be satisfied. The trajectory of μ as a function of r is shown in Fig. 5 for $c_1=0.71$, corresponding to a temperature below melting. There is now a range of μ over which the derivative term is negative enough. It is obvious that our condition can be satisfied. This illustrates that the transition temperature is lower than the bulk melting temperature. We next study the dependence of the melting condition on the radius R of the sphere.

In general, both c_1 and c_1'' are functions of the temperature. Unfortunately not much experimental information exists on c_1''. As an approximation, we have used the Wertheim[29] analytic solution of the Percus-Yevick[30] equation of the hard-sphere fluid to determine both c_1 and c_1'' for different hard-sphere radii σ. c_1'' is then fitted as a polynomial of c_1 in the range $0.015<c_1<0.89$ as

$$c_1''=-0.049\,00-0.995\,79c_1-0.035\,440c_1^2 -0.044\,14c_1^3-0.001\,51c_1^4 .$$

In Fig. 6 we show the dependence Δc_{1m} as a function of $1/R$. In the limit of large R we expect Δc_1 to depend linearly on $1/R$. There is deviation from this scaling behavior at small R, however.

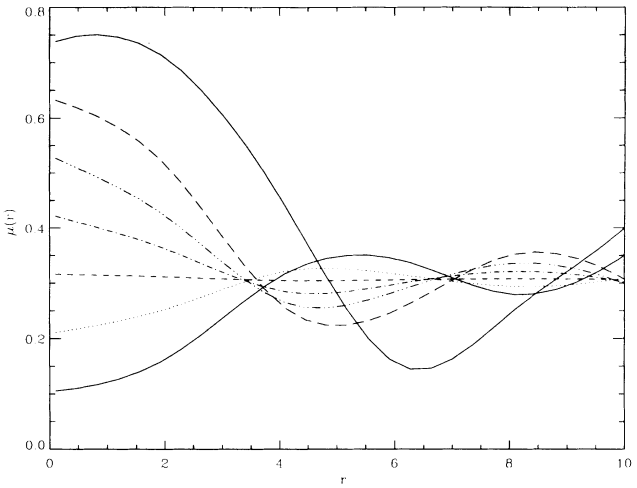

FIG. 5. The trajectory of μ as a function of r for a spherical cluster for various initial values $\mu(r=0)$. $c_1=0.71$, corresponding to a temperature below melting.

The trajectories $\mu_m(r/R)$ consists of a flat bulklike part close to the center and a decaying interface part at the surface. For small particles ($R=5$), the surface part dominates. For larger R ($R=10$ and 15), the trajectories are similar for different values of R. This is illustrated in Fig. 7. The average value of μ provides a measure of the mean-squared lattice vibration amplitude through μ. This quantity can be measured by Mössbauer spectroscopy or by x-ray-type measurements. This represents a type of generalized Lindemann criterion for small clusters.

A model of melting in small clusters consists of different nuclei first forming at the surface of the boundary. These nuclei eventually coalesce with grain boun-

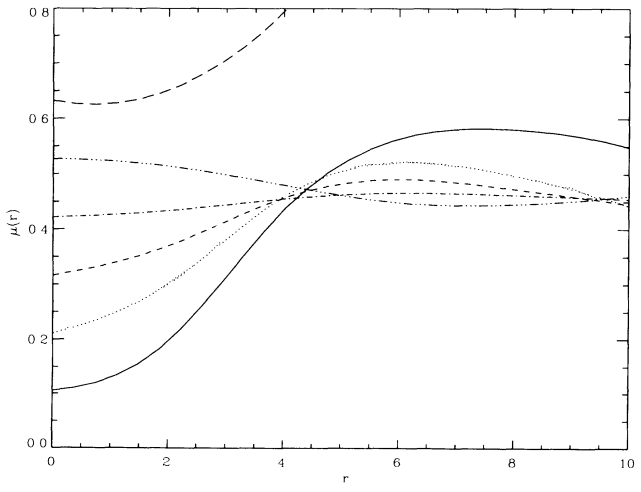

FIG. 4. The trajectory of μ as a function of r for a spherical cluster for various initial values $\mu(r=0)$. $c_1=0.66$, corresponding to a temperature near melting.

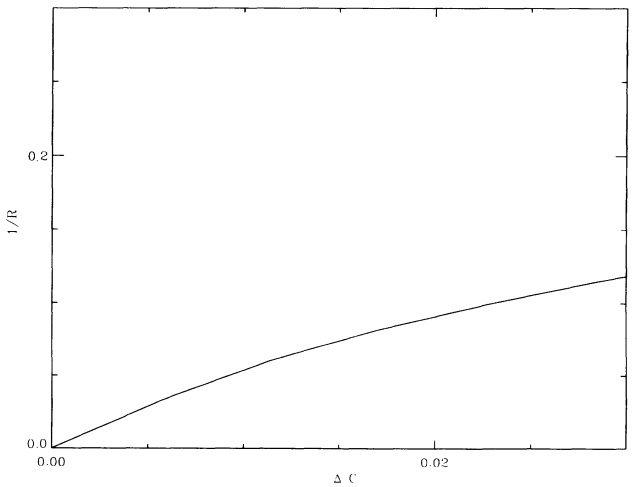

FIG. 6. The dependence Δc_{1m} as a function of $1/R$ with distances expressed in units of the lattice constant.

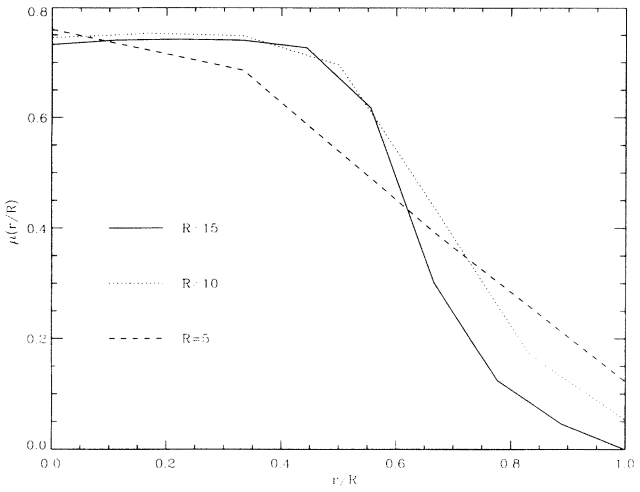

FIG. 7. The trajectories of the order parameter for different cluster radii R. $\mu_m(r/R)$ are similar for different values of R for $R=10$ and 15.

daries formed between them. This is a dynamical question. Here we have investigated situations that are locally stable, subject to certain boundary conditions. Multidomain situations correspond to the order parameters μ that are not spherically symmetric and have not been investigated here.

There have been recent discussions of surface melting. In the present picture, surface melting occurs when μ becomes zero at the boundary but remains finite close to the origin.

In the picture that we have developed here, whether the pores may be connected is not a very important issue because the order parameter is already close to zero at the boundary.

V. MELTING OF FILMS

Finally, we study the melting of thin films. We consider the case of a thin film confined by two walls a distance d apart. To be specific, we consider the case such that the (001) face of the bcc crystalline phase is in contact with the wall. There are two groups of order parameters which we call μ_1 and μ_2, corresponding to the smallest RLV parallel $[(\pm1,\pm1,0)2\pi/a]$ and nonparallel $[(\pm1,0,\pm1)2\pi/a]$, $[0,\pm1,\pm1)2\pi/a)]$ to the walls. We pick a set of coordinates so that the origin is at the center of the film and the walls are at $\pm d/2$.

In contrast to the cluster case, the boundary conditions are now different. Again, we expect the mass density to be zero outside the walls and thus $\rho(d/2+a)=0$. This condition can now be satisfied if $\cos[(d/2+a)K]=0$, even if $\mu(z=d/2+a)\neq0$, because ρ is related to the product of the two. Because of the presence of the wall, we expect the mean-squared lattice vibration in the z direction to be much smaller than that along directions parallel to the plane. Recall that the order parameter is the exponential of the mean-squared lattice vibration, i.e., $\mu_j=\exp[-K_j^2\langle(\delta r_j)^2\rangle]$. As we can see from Fig. 2, because of the sharpness of the first peak of $\rho(z)$ compared with that of $S_K(z)$, $\langle(\delta z)^2\rangle\ll\langle(\delta r_\parallel)^2\rangle$. We thus expect approximately $\mu_1(z=d/2)=\exp[-K^2\langle(\delta a r_\parallel)^2\rangle]$, $\mu_2(z=d/2)=\exp[-K_\parallel^2\langle(\delta r_\parallel)^2\rangle]$, and $\mu_1(z=d/2)=\mu_2(z=d/2)^\alpha$ where $\alpha=(K_\parallel/K)^2$; $K_\parallel$ is the component of the nonparallel RLV that is parallel to the surface. For the 001 face of a bcc lattice $\alpha=0.5$. We also expect the interface profile to be symmetric with respect to its center at $z=0$. Hence $\mu'(z=0)=0$.

The corresponding differential equations are now

$$\mu_1=F_1(c_1\mu_1,c_1\mu_2+D\mu_2)\ ,$$

$$\mu_2=F_2(c_1\mu_1,c_1\mu_2+D\mu_2)\ ,$$

where $D\mu_2=-0.25c_1''\mu_2''$. We assume that the order parameter does not change parallel to the interface. Thus only the derivative of μ_2 appears. Also, RLV's that are not parallel to the wall are at 45° with respect to the normal. Thus an extra factor of $\frac{1}{2}$ appears in $D\mu_2$. The dependence on the derivative terms $D\mu_2$ can be eliminated by combining the first and second equations. We obtain a relationship between μ_2 and μ_1. This relationship has been solved numerically and is shown in Fig. 8. We found that $\mu_1=\mu_2$ at $c_1=c_{1m}$ while for $c_1<c_{1m}$, $\mu_2>\mu_1$. We again solve the boundary value problem with the shooting method by starting with different initial values with zero initial slope at the center and ask whether the corresponding boundary condition at the wall can be satisfied.

Typical trajectories are similar to those discussed in the preceding section. A typical set of μ_1 as a function of z are shown in Fig. 9 at a temperature below the bulk transition temperature. We take the left-hand side of this graph ($z=-10$) to be the center. We start off with different μ's with zero initial slope according to our boundary condition. The different initial values of μ can be read off from the left-hand side of the graph. Similar to what we pointed out in the preceding section, when μ is close to 0.5, it changes slowly. The lowest-energy

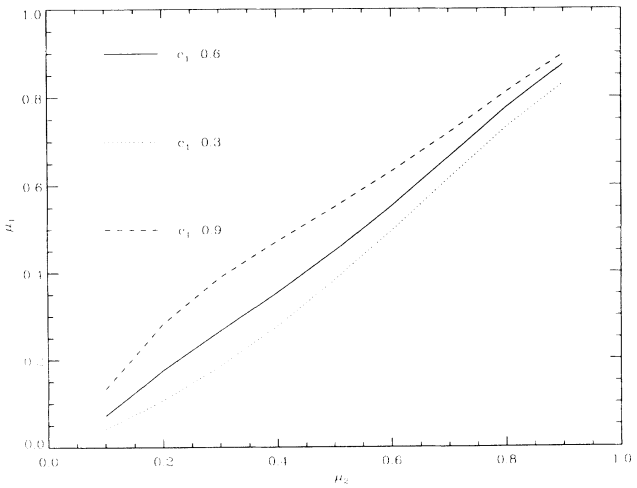

FIG. 8. The in-plane order parameter μ_2 as a function of the out-of-phase order parameter μ_1 for various values of c_1.

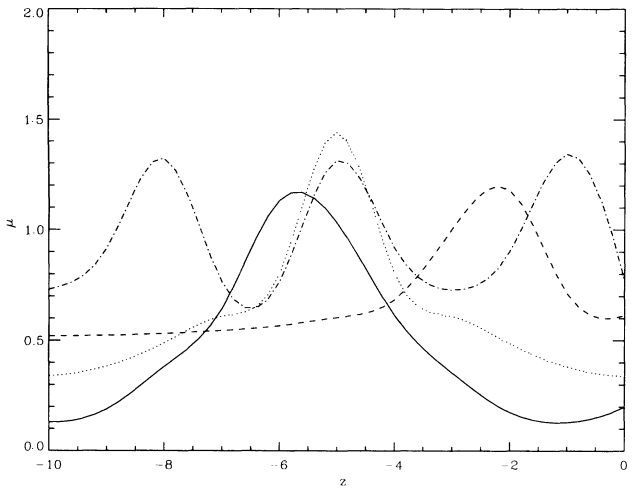

FIG. 9. Typical trajectories of μ_1 as a function of z are shown at a temperature below the bulk transition temperature for different initial values μ_1 at the center of the film $z=-10$ when $d\mu/dz=0$. $c_1=0.648$.

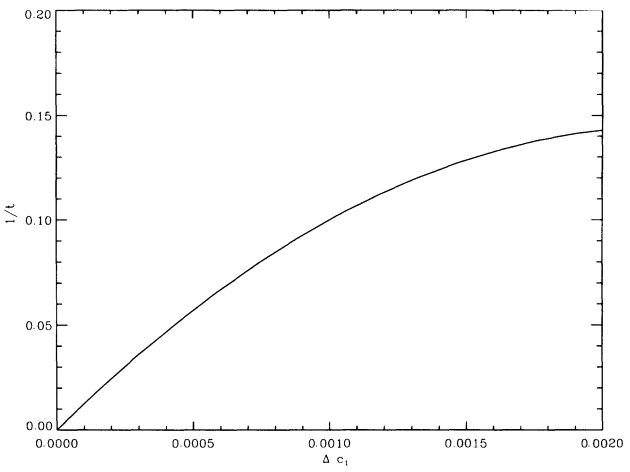

FIG. 10. The shift in c_1 as a function of the inverse of half of the film thickness $1/t$ in units of the lattice constant.

configuration corresponds to μ exhibiting less than one oscillation inside the film. Those with more than one oscillation correspond to a multidomain structure. Our boundary condition at the surface, $\mu_1=\mu_2^{\alpha}$, can be satisfied only if μ is close to 1, corresponding to a highly ordered situation at the wall. Figure 9 can be used for films of different widths by reading off from this graph the values of μ at different values of z. For a film with half-width 4, this boundary condition can only be satisfied for an initial value at the center close to 0.1 with a value of around 1 at the wall, corresponding to the solid line in Fig. 9. The order parameter is larger at the walls than at the center. This result is consistent with computer simulations[31,32] which indicate much stronger layering tendency close to a wall. The melting temperature is determined as the lowest temperature below which the boundary condition at $z=d/2$ can no longer be satisfied. The above trajectories thus illustrate that the melting temperature is increased. In Fig. 10, we show the shift in c_1 as a function of the inverse of half of the film thickness $1/t$.

Experimentally Devaud and Willens[33] reported a suppression of the melting temperature in Pb-Ge films. Sevenhans *et al.*[34] were unable to observe the melting for films of the same chemical composition. They found that the layered structure was destroyed by the crystallization that occurs substantially below the melting temperature. Recently Unruh *et al.*[14] have been able to fabricate a multilayer structure of copper and tungsten so that the tungsten layers remain solid and well defined while the copper layers melt. Their results suggest that the melting temperature is increased, as we found here.

In conclusion, we have studied the melting of clusters and thin films by generalizing recent density-functional methods of melting. We found that the freezing temperature, as well as the mean-squared vibrational amplitude, is decreased for thin films whereas for clusters it is enhanced. We found that at melting the Debye-Waller factors as a function of the radial distance are very similar after a scaling by the cluster radius R for different cluster sizes R. The present technique is one of the few ways by which one can obtain quantitative information for systems of intermediate sizes of the order of 10 000 particles for which it is impractical to carry out Monte Carlo simulations.

ACKNOWLEDGMENTS

This research is supported by the Office of Naval Research Grant No. N00014-88-K-0003. We thank J. Beamish, C. L. Chien, P. Sheng, and K. Unruh for helpful discussions.

APPENDIX

For x between 0 and 1, the functions $g(x)$ and $f_j(x)$ can be fitted very well by the exponential of a polynomial as $\exp(\sum_{n=1}^{3}a_n x^{n-1})$ where a_n are constants. On the other hand, the function F and its inverse, F^{-1}, can be fitted simply by a polynomial; the exponential dependence of f and g cancels out. For a bcc lattice, retaining the lowest reciprocal-lattice vectors, assuming that all the μ_j's are equal and $c_0=-40$ we found that for a third-order polynomial, $F^{-1}(x)=-0.0033+1.050\,87x-1.502\,14x^2+1.403\,43x^3$ with a normalized root-mean-square error of 0.0068 while for a fourth-order polynomial $F^{-1}(x)=0.000\,65+0.883\,44x-0.669\,80x^2+0.113\,21x^3+0.622\,36x^4$ with a normalized root-mean-square error of 0.0018.

The solution of Eq. (5) is illustrated in Fig. 1 where we have plotted $F^{-1}(x)$ vs x. For a small c_1 (high temperature) the curve $F^{-1}(x)$ does not intersect the line A given by $y=c_1x$. The melting transition occurs when the straight line B is tangent to the curve. This is analogous to the Weiss mean-field model of magnetism. However, in contrast to that case, the point of contact first occurs at a finite μ, consistent with a first-order transition. For this to occur, it is important for the curve F^{-1} to be

fitted with a polynomial with a degree higher than the third. Just as in previous calculations[12] we found that for $c_1=0.687$, the transition occurs at $\mu=0.7$; however, the minimum value of c_1 at which the transition first occurs is at $c_1=0.65$. We note that the curve F^{-1} is nearly parallel to the curve $y=c_1\mu$ and the precise determination of μ_m can be difficult. We have changed the number of points in the Gauss-Lagrange formula as well as the degree of the interpolating polynomial. This minimum value of c_{1m} changes by less than 1%.[35]

[1]P. Pawlow, Z. Phys. Chem. **65**, 545 (1909).
[2]M. Takagi, J. Phys. Soc. Jpn. **9**, 359 (1954).
[3]Ph.-A. Buffat and J. P. Borel, Phys. Rev. A **13**, 2287 (1970).
[4]T. Matsubara, Y. Iwase, and A. Momkita, Prog. Theor. Phys. **58**, 1102 (1977).
[5]M. Hasegawa, K. Hoshino, and M. Watabe, J. Phys. F **10**, 619 (1980).
[6]J. D. Weeks, D. Chandler, and H. C. Andersen, J. Chem. Phys. **54**, 5237 (1971).
[7]P. Sheng, R. W. Cohen, and J. R. Schrieffer, J. Phys. C **14**, L565 (1981).
[8]J. E. Lennard-Jones and A. F. Devonshire, Proc. R. Soc. London, Ser. A **170**, 464 (1939).
[9]S. T. Chiu, Phys. Rev. B **28**, 178 (1983).
[10]J. M. Kosterlitz and D. Thouless, J. Phys. C **6**, 1181 (1973).
[11]L. K. Moleko and H. R. Glyde, Phys. Rev. B **30**, 4215 (1984).
[12]T. V. Ramakrishnan and M. Yussouff, Phys. Rev. B **19**, 2775 (1958). This type of approach is called the density-functional method because the potential is related to the change in density as a kind of functional derivative.
[13]J. G. Kirkwood and E. Monroe, J. Chem. Phys. **9**, 514 (1941).
[14]K. Unruh, B. M. Patterson, S. I. Shah, G. A. Jones, Y. W. Kim, and J. E. Greene, in *TITLE,* edited by EDITORS, MRS Symposia Proceedings No. 132 (Materials Research Society, Pittsburgh, 1989), p. 225.
[15]H. J. Raveche and R. G. Kayser, J. Chem. Phys. **68**, 3632 (1978).
[16]J. D. Weeks, S. A. Rice, and J. J. Kozak, J. Chem. Phys. **52**, 2416 (1970).
[17]W. A. Curtin and N. W. Ashcroft, Phys. Rev. Lett. **56**, 2775 (1986).
[18]K. S. Liu, M. H. Kalos, and G. V. Chester, Phys. Rev. A **10**, 303 (1974).
[19]F. Abraham and Y. Singh, J. Chem. Phys. **67**, xx (1977).
[20]I. Snook and D. Henderson, J. Chem. Phys. **68**, 2134 (1978).
[21]D. Henderson, F. F. Abraham, and J. A. Barker, Mol. Phys. **31**, 1291 (1976).
[22]W. F. Samm and C. Ebner, Phys. Rev. A **17**, 1768 (1978).
[23]W. McMullen and D. Oxtoby, J. Chem. Phys. **88**, 1967 (1988).
[24]S. T. Chui, Phys. Rev. B **43**, 11 523 (1991).
[25]S. T. Chui, Phys. Rev. B **43**, 10 654 (1991).
[26]D. W. Oxtoby and A. D. J. Haymet, J. Chem. Phys. **76**, 6262 (1982).
[27]A. J. M. Yang, P. D. Fleming III, and J. H. Gibbs, J. Chem. Phys. **64**, 3732 (1976).
[28]P. Harrowell and D. W. Oxtoby, J. Chem. Phys. **80**, 1639 (1984).
[29]M. S. Wertheim, Phys. Rev. Lett. **10**, 321 (1963).
[30]J. K. Percus and G. J. Yevick, Phys. Rev. **110**, 1 (1958).
[31]S. Toxvaerd, J. Chem. Phys. **74**, 1998 (1981).
[32]J. Q. Broughton, A. Bonissent, and F. F. Abraham, J. Chem. Phys. **74**, 4029 (1981).
[33]G. Devaud and R. H. Willens, Phys. Rev. Lett. **57**, 2683 (1986).
[34]W. Sevenhans, J.-P. Locquet, Y. Bruynseraede, H. Homma, and I. K. Schuller, Phys. Rev. B **38**, 4974 (1988).
[35]V. Privman and M. E. Fisher, J. Stat. Phys. **33**, 385 (1983).